Performance of an Adaptive Multiuser OFDM Uplink With Carrier Frequency Offsets

Wei Wang, Tony Ottosson and Tommy Svensson
Dept. Signals and Systems, Chalmers University of Technology, SE-412 96 Göteborg, Sweden
{wei.wang, tony.ottosson, tommy.svensson}@chalmers.se

Abstract

Using an OFDM based uplink for the future cellular network has been a controversial issue due to difficulties in time and frequency synchronization and high Peak-to-Average Power Ratio (PAPR). In this paper, a model is provided to quantify the effects of carrier frequency offsets in a multiuser OFDM uplink. We propose a slotted OFDM radio interface, in which time-frequency bins are allocated adaptively to different users based on their channel conditions. Frequency division duplex (FDD) is assumed, which enables the feedback of synchronization and scheduling information. The theoretical evaluations show that the attainable spectral efficiency highly depends on the carrier frequency offset. The results indicate that the loss in spectral efficiency is small with no more than 2% carrier frequency offset of the subcarrier spacing.

I. Introduction

In a broadband multiuser environment, an orthogonal frequency division multiplexing (OFDM) based system has strong potential in attaining high spectral efficiency, particularly for the downlinks [1], [2], [3]. It has the advantage in using low complexity frequency-domain equalizers if the channel does not change much during one OFDM symbol. It also provides fine granularity so that multiple users may share the total bandwidth to multiplex their data in both time and frequency.

However, it is not apparent that OFDM would be an appropriate solution in the multiuser uplink scenario. Accurate uplink multiuser time and frequency synchronization is a challenging task. Furthermore, high Peak-to-Average Power Ratio (PAPR) leads to more power consumption. In [4], an adaptive single-carrier TDMA based uplink with decision feedback frequency-domain equalizer has been proposed. It is shown in [4] that the attainable spectral efficiency is not satisfactory due to limited multiuser diversity gain. In this paper, we take a closer look into a multiuser OFDM uplink by taking into consideration the carrier frequency offset.

To achieve a consistent data structure as in the downlink[1], we assume the following target system parameters:

- time-frequency bins of size 0.667 ms and 200 kHz;
- symbols and cyclic prefix of length 100μs and 11μs, respectively;
- a subcarrier spacing of 10 kHz.

The resulting time-frequency bin thus carries 120 symbols, with 6 symbols of length 111μs on each of the 20 subcarriers. Out of the 120 symbols, 12 are for training and downlink control, leaving 108 payload symbols, see Fig. 1.

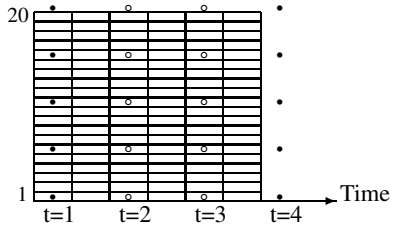

Fig. 1. One time-frequency bin contains 20 subcarriers with 6 symbols each. Known 4-QAM pilot symbols (black) and 4-QAM control data symbols (rings) are placed on four pilot subcarriers. The modulation format for the other (payload) symbols is adjusted adaptively. The bin is assumed to be exclusively allocated to one out of K users. All payload symbols within a bin use the same modulation format.

Channel estimation and prediction play an important role in an adaptive multiuser packet transmission. It requires channel knowledge of all the uplink users in order to allocate the resources. To limit the amount of pilot overhead, a Kalman estimator and predictor with overlapping pilots are studied in [5]. It efficiently utilizes the time and frequency channel correlation and meets the accuracy requirement of an adaptive transmission loop. The base station predicts the Signal to Interference and Noise Ratio (SINR) for all bins of all the users 3 time-slots ahead. A simple scheduler then allocates each upcoming time-frequency bin to the user who can utilize the channel best with the appropriate modulation format. The decisions are signaled back in the downlink transmission time-slot. As a result, the spectral efficiency will increase with the number of active users.

The performance of an uplink multiuser system depends closely on the carrier frequency, sampling clock frequency and symbol time synchronization accuracy. As long as the cyclic prefix is longer than the sum of the symbol time offset and the length of the channel impulse response, the rotation due to symbol time synchronization errors and the phase shifts caused by the channel together can be taken care of by the channel estimator. Sampling clock frequency errors below 10ppm have little impact on the system performance [6], [8]. Carrier frequency synchronization errors will cause

[1]More details, especially on the cellular aspects of the proposal, can be found in the companion papers [2] and [3].

Inter-Carrier-Interference (ICI) and hence is harmful in terms of Symbol Error Rate (SER). Paper [7] suggests a time and frequency synchronization scheme by utilizing the cyclic prefix, which satisfies the synchronization requirements. The estimation is performed at the base station and the control information is fed back in the downlink to the users to adjust their symbol clocks and oscillators.

II. Effects of Frequency Offsets in Multiuser OFDM Uplink

The model derived in [8] quantifies the impact of frequency synchronization errors without including the effects of FFT demodulator. As a consequence, interference experienced by the different uplink subcarriers vary. In this paper, we propose a model which analyzes the frequency synchronization errors after the FFT demodulation process at the receiver, which yields a closed form solution to quantify the variance of the ICI.

A. Analysis

We consider an OFDM system of N equally spaced subcarriers and bandwidth B_{OFDM}. The uncoded transmitted symbol at the lth subcarrier f_l of the mth OFDM symbol is denoted as $D_m(l)$. The transmitted OFDM symbol can be expressed in the form

$$\begin{aligned} s_m(t) &= \frac{1}{\sqrt{N}} \sum_{l=0}^{N-1} D_m(l) e^{j2\pi f_l t} \\ & \quad t \in [mT_{OFDM}, (m+1)T_{OFDM}] \end{aligned} \tag{1}$$

where T_{OFDM} is the OFDM symbol period without the cyclic prefix and $f_l = \frac{l}{T_{\text{OFDM}}}$.

The following assumptions have been made to ease the analysis of the effects of the uplink carrier frequency offset:

- the uplink users are perfectly synchronized in OFDM sampling time and symbol time;
- a special case where each uplink user occupies one unique subcarrier is considered;
- no guard-band is allocated between different users.

The received signal with carrier frequency offset $\Delta\hat{f}_l$ for the lth subcarrier is written as

$$r_m(t) = \frac{1}{\sqrt{N}} \sum_{l=0}^{N-1} H_m(l) D_m(l) e^{j2\pi f_l t} e^{j2\pi \Delta\hat{f}_l t} + w(t), \tag{2}$$

where $H_m(l)$ is the frequency response of the channel over the lth subcarrier at the mth OFDM symbol and $w(t) \sim N(0, \sigma^2)$. We assume that the channel is constant over one OFDM symbol period T_{OFDM}. The carrier frequency offset for each subcarrier is independent and identically Gaussian distributed, $\Delta\hat{f}_l \sim N(0, \hat{\sigma}_f^2)$.

By sampling the received signal $r_m(t)$ with period $T = \frac{T_{OFDM}}{N}$, we obtain the discrete form signal

$$r_m(nT) \doteq r_m(n) = \frac{1}{\sqrt{N}} \sum_{l=0}^{N-1} H_m(l) D_m(l) e^{j2\pi ln/N} e^{j2\pi \Delta f_l n} + w(n). \tag{3}$$

where $\Delta f_l = \Delta\hat{f}_l T$ and $\Delta f_l \sim N(0, \sigma_f^2)$, $\sigma_f = \hat{\sigma}_f T$ consequently.

The kth subcarrier is demodulated by taking the FFT at the kth index

$$\begin{aligned} R_m(k) &= \frac{1}{\sqrt{N}} \sum_{n=0}^{N-1} r_m(n) e^{-j2\pi kn/N} \\ &= \frac{1}{N} \sum_{n=0}^{N-1} \sum_{l=0}^{N-1} H_m(l) D_m(l) e^{j2\pi(l-k)n/N} e^{j2\pi \Delta f_l n} + W(k) \\ &= \underbrace{\frac{1}{N} H_m(l) D_m(l) \sum_{n=0}^{N-1} e^{j2\pi \Delta f_l n}}_{l=k} \\ &\quad + \frac{1}{N} \sum_{n=0}^{N-1} \sum_{\substack{l=0 \\ l \neq k}}^{N-1} H_m(l) D_m(l) e^{j2\pi(l-k)n/N} e^{j2\pi \Delta f_l n} \\ &\quad + W(k), \end{aligned} \tag{4}$$

where $W(k)$ is the FFT of $w(n), n = 0, \ldots, N-1$. The first term is the desired symbol $D_m(l)$ rotated and scaled by a common factor $\frac{1}{N} H_m(l) \sum_{n=0}^{N-1} e^{j2\pi \Delta f_l n}$. The second term is the interference that causes ICI and corrupts the wanted symbol. Here we focus on the second term and denote it as ICI. Furthermore, we assume the carrier frequency offset $\Delta f_l N \ll 1$. Therefore we can substitute the frequency offset term with the first order Taylor expansion

$$e^{j2\pi \Delta f_l n} \approx 1 + j2\pi \Delta f_l n. \tag{5}$$

and rewrite the ICI term as

$$\begin{aligned} \text{ICI} &= \frac{1}{N} \sum_{n=0}^{N-1} \sum_{\substack{l=0 \\ l \neq k}}^{N-1} H_m(l) D_m(l) e^{j2\pi(l-k)n/N} e^{j2\pi \Delta f_l n} \\ &\approx \frac{1}{N} \sum_{n=0}^{N-1} \sum_{\substack{l=0 \\ l \neq k}}^{N-1} H_m(l) D_m(l) e^{j2\pi(l-k)n/N} (1 + j2\pi \Delta f_l n) \\ &= \underbrace{\frac{1}{N} \sum_{n=0}^{N-1} \sum_{\substack{l=0 \\ l \neq k}}^{N-1} H_m(l) D_m(l) e^{j2\pi(l-k)n/N}}_{=0} \\ &\quad + j\frac{2\pi}{N} \sum_{n=0}^{N-1} \sum_{\substack{l=0 \\ l \neq k}}^{N-1} H_m(l) D_m(l) e^{j2\pi(l-k)n/N} \Delta f_l n \\ &= j\frac{2\pi}{N} \sum_{n=0}^{N-1} \sum_{\substack{l=0 \\ l \neq k}}^{N-1} H_m(l) D_m(l) e^{j2\pi(l-k)n/N} \Delta f_l n. \end{aligned} \tag{6}$$

The ICI term is a sum of a large number of zero mean independent and identically distributed random variables, which can be modeled as a complex Gaussian random variable with zero mean and variance

$$E[|\text{ICI}|^2] = \frac{4\pi^2}{N^2} E[(\sum_{\substack{l=0 \\ l\neq k}}^{N-1} H_m(l) D_m(l) \Delta f_l \sum_{n=0}^{N-1} e^{j2\pi(l-k)n/N} n) \times (\sum_{\substack{q=0 \\ q\neq k}}^{N-1} H_m(q)^* D_m^*(q) \Delta f_q \sum_{v=0}^{N-1} e^{-j2\pi(q-k)v/N} v)] \quad (7)$$

Since $D_m(l)$ and $D_m(q)$ are independent, product in (7) is nonzero when $l = q$. We denote E_S as the symbol energy and σ_f^2 as the variance of carrier frequency offset of each user. Assuming a normalized channel, $E[|H_m(l)|^2] = 1$, (7) becomes

$$E[|\text{ICI}|^2] = \frac{4\pi^2}{N^2} E_s \sigma_f^2 \sum_{n,v=0}^{N-1} \sum_{\substack{l=0 \\ l\neq k}}^{N-1} e^{j2\pi(l-k)(n-v)/N} nv \quad (8)$$

where the sum

$$\sum_{\substack{l=0 \\ l\neq k}}^{N-1} e^{j2\pi(l-k)(n-v)/N} = \begin{cases} N-1 & n = v, \\ -1 & otherwise. \end{cases} \quad (9)$$

Finally, the variance of the ICI becomes

$$\sigma_{\text{ICI}}^2 = E[|\text{ICI}|^2] = \frac{4\pi^2}{N^2} E_s \sigma_f^2 [(N-1) \sum_{n=0}^{N-1} n^2 - \sum_{n,v=0}^{N-1} nv] = \frac{\pi^2 E_s \sigma_f^2 (N^2-1)}{3} \quad (10)$$

Based on (10), we define the SINR as

$$\text{SINR} = E_s / (\sigma^2 + \sigma_{\text{ICI}}^2), \quad (11)$$

and Signal-to-Interference Ratio (SIR) as

$$\text{SIR} = E_s / \sigma_{\text{ICI}}^2. \quad (12)$$

Fig. 2 shows the SIR with different carrier frequency offsets. This ratio determines the irreducible symbol error floor of a certain modulation format.

B. Simulations

Simulations are needed to validate the model. Besides the assumptions in II-A, the carrier frequency offsets also change from one OFDM symbol to the other.

In Fig. 3 and Fig. 4, both analytical and simulated symbol error rates are presented in the case of 2% carrier frequency offset. We notice that there is a discrepancy between the analytical and simulated symbol error rate in Fig. 4 when the symbol error rate approaches the noise floor. This difference comes from the Gaussian assumption we made during the analysis. We calculate the pdf of the real part of the ICI term of an OFDM system with 256 subcarriers in the presence of 2% carrier offset and present it in Fig. 5, which is not perfectly Gaussian. *In the final version of this paper, we will further investigate the effects of carrier frequency errors by validating the Gaussian assumption of the ICI term.*

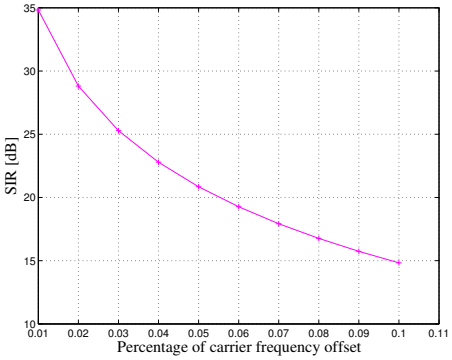

Fig. 2. Signal-to-interference ratio due to carrier frequency offset.

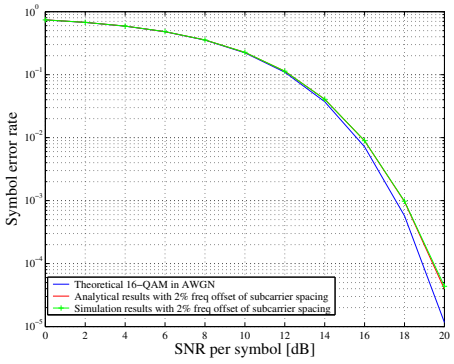

Fig. 3. Symbol error rate of 16-QAM over AWGN channel with 2% carrier offset. The OFDM system has 512 subcarriers.

C. Bin-based OFDM

In a bin-based multiuser uplink scenario, we further assume that the carrier frequency offset is constant within one user's group of subcarriers within a bin. Therefore $\Delta \hat{f}_l$ is correlated over time. However, since the symbols $D_m(l)$ transmitted inside the bin are independent, no cross-term within the bin will be seen in (7). Hence the variance of ICI in a bin-based OFDM can be expressed by (10).

III. Analysis on the Spectral Efficiency

For the analysis we assume independent Rayleigh fading between bins and time-invariant flat AWGN channels within bins. Equal average received power from all the users is assumed at the base station. Channels from different users fade independently.

The spectral efficiency in each time-slot is calculated as follows

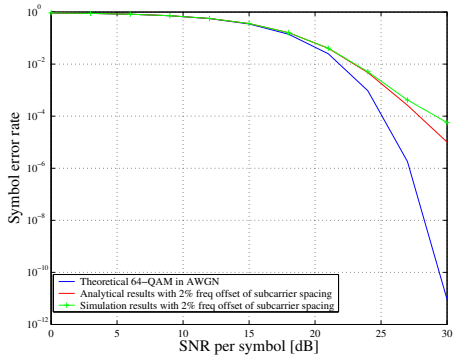

Fig. 4. Symbol error rate of 64-QAM over AWGN channel with 2% carrier offset. The OFDM system has 512 subcarriers.

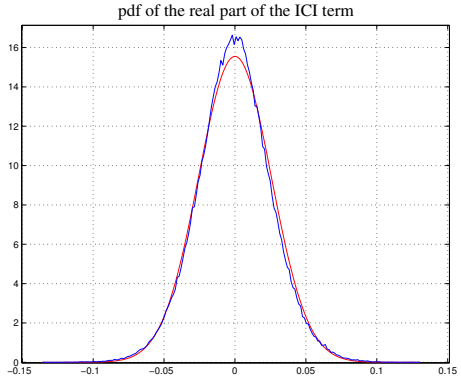

Fig. 5. Pdf of of real part of the ICI term of an OFDM system with 256 subcarriers in the presence of 2% carrier offset. The modulation format is 16-QAM.

$$\eta(\gamma) = G_c G_p \max\left\{k_i(1 - P_{f,i}(\gamma))\right\} \quad \text{bits/s/Hz} . \tag{13}$$

Here, k_i is the number of bits per symbol using uncoded 2^{k_i}-ary QAM modulation. $G_c = 100/111$ is due to the cyclic prefix and $G_p = 108/120$ is due to the 12 pilots and control symbols per bin. Moreover, $P_{f,i}(\gamma)$ is the frame error rate for the modulation level i. These frame error rates can be calculated as

$$P_{f,i}(\gamma) = 1 - (1 - P_{e,i}(\gamma))^{108}, \tag{14}$$

where $P_{e,i}(\gamma)$ is the symbol error rate for level i when 2^{k_i}-ary QAM is used in a SINR region $[\gamma_i, \gamma_{i+1})$, $\gamma_L = \infty$. The exponent 108 represents the number of payload data symbols. The adaptive modulation scheme is optimized to maximize the throughput including also the ARQ part of the transmission. The thresholds γ_i, obtained by using the analytical expressions for $P_{e,i}(\gamma)$, are given in Table I.

For flat Rayleigh fading, the pdf $p(\gamma)$ resulting from the selection diversity of the K active users, is expressed as

$$p(\gamma) = \frac{K}{\bar{\gamma}}(1 - e^{-\gamma/\bar{\gamma}})^{K-1} e^{-\gamma/\bar{\gamma}}, \tag{15}$$

TABLE I

SWITCHING LEVELS γ_i

i	Modulation	k_i	γ_i (dB)
0	BPSK	1	$-\infty$
1	4-QAM	2	8.701
2	8-PSK	3	14.58
3	16-QAM	4	16.84
4	32 Cross-QAM	5	20.46
5	64-QAM	6	23.59
6	128 Cross-QAM	7	26.86
7	256-QAM	8	29.94

where $\bar{\gamma}$ is the average received SINR of each user. The average spectral efficiency is then calculated as

$$\eta = G_c G_p \sum_{i=0}^{L-1} k_i \int_{\gamma_i}^{\gamma_{i+1}} (1 - P_{f,i}(\gamma)) p(\gamma)\, d\gamma \quad \text{bits/s/Hz} . \tag{16}$$

Higher modulation formats might not contribute to the spectral efficiency due to the noise floor introduced by carrier frequency offsets. For example, 256-QAM might be unnecessary in the case of carrier frequency offset 2% of subcarrier spacing. One can also cutoff at 32-QAM when the carrier frequency offset is 5% of subcarrier spacing.

Numerical evaluations are as presented in Fig. 6 at SNR = 16 dB. The gain in multiuser diversity is evident. In the presence of small carrier frequency offset, the loss in spectral efficiency is small. However, a 5% offset of subcarrier spacing leads to a considerable loss in spectral efficiency. Lower modulation formats are chosen due to a higher degradation in the received SINR.

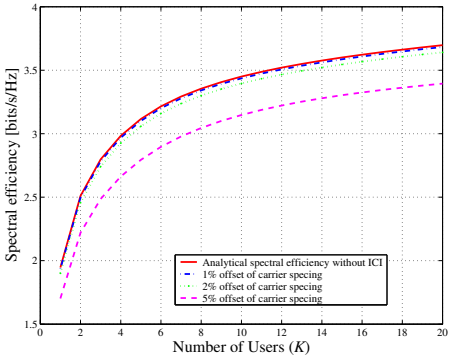

Fig. 6. Spectral efficiency at SNR 16 dB. It increases with the number of users in the system. Carrier frequency offset of 1%, 2% and 5% subcarrier spacing are presented together with the spectral efficiency obtained by an adaptive uplink multiuser OFDM system without frequency synchronization errors.

IV. SIMULATION RESULTS

We will relax the assumptions about the channel and instead generate a frequency-selective channel with variations within a bin. A loss in spectral efficiency is expected due to variations. We still however assume perfect knowledge of the channel. Since the ICI is modeled as a complex Gaussian random

variable with variance σ^2_{ICI}, it is equivalent to perform the simulations at an effective SINR $= E_s/(\sigma^2 + \sigma^2_{\text{ICI}})$.

The assumed system is operating at carrier frequency 1900 MHz with 5 MHz bandwidth that is divided into 500 subcarriers. The modified ITU-IV Channel A power delay profile is used and given in Table II. The speed of the terminals is 50 km/h.

TABLE II

POWER DELAY PROFILES

	ITU-IV Channel A	
Tap	Relative delay [ns]	Average power [dB]
1	0	0
2	400	-1.0
3	800	-9.0
4	1000	-10.0
5	1800	-15.0
6	2600	-20.0

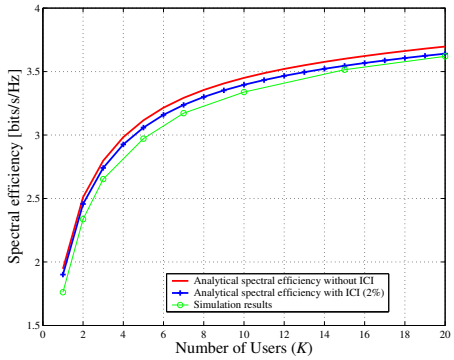

Fig. 7. Simulation results at SNR 16 dB with carrier frequency offset of 2% subcarrier spacing are presented together with the analytical values.

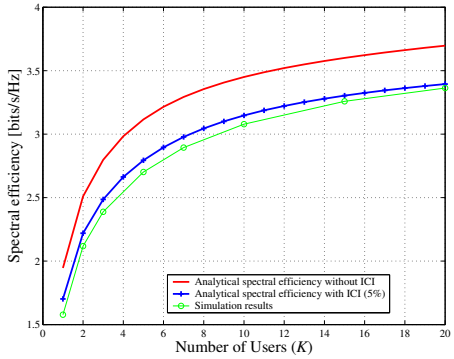

Fig. 8. Simulation results at SNR 16 dB with carrier frequency offset of 5% subcarrier spacing are presented together with the analytical values.

In the simulations, the channels are no longer time-invariant within the bins. Therefore the actual frame error rate is calculated as $P^*_{f,i}(\gamma) = 1 - \prod_j (1 - P_{e,i,j}(\gamma_j))$. Here $P^*_{f,i}(\gamma)$ denotes the actual frame error rate for the modulation level i. The index j is the payload symbol number and γ_j is the instantaneous SINR of the j_{th} payload symbol. $P_{e,i,j}(\gamma_j)$ denotes the symbol error rate of the j_{th} payload symbol for modulation level i. With the actual frame error rate, one can recalculate the spectral efficiency in each bin as (13).

The lower instantaneous SINRs in the bin essentially determine the symbol error rate and consequently the overall spectral efficiency of the bin. Simulation results are presented in Fig. 7 and Fig. 8. The symbol error rate formulas of 32 Cross-QAM and 128 Cross-QAM used to calculate the thresholds and frame error rate are the upper bounds [9]. An upper bound of symbol error rate leads to a underestimated analytical spectral efficiency. These two modulation formats occurs frequently when the number of users is high in the system. Therefore the simulated spectral efficiency grows closer to the analytical values with the increase of the number of users.

V. CONCLUSIONS

In this paper, we evaluate the performance of an adaptive OFDM based uplink with carrier frequency errors. An analytical model is derived to quantify the effects of carrier frequency offsets. The results show that a frequency accuracy of 1% - 2% of the subcarrier spacing is necessary to obtain the spectral efficiency close to the corresponding downlink system. However, even with a carrier frequency offset as high as 5% of the subcarrier spacing, the result is still outperforming an adaptive single-carrier TDMA system.

VI. ACKNOWLEDGMENT

The authors would like to thank Florent Munier for the fruitful discussion in the subject of OFDM with frequency offsets.

REFERENCES

[1] Online: www.signal.uu.se/Research/PCCwirelessIP.html.

[2] W. Wang, T. Ottosson, M. Sternad, A. Ahlén and A. Svensson, "Impact of Multiuser Diversity and Channel Variability on Adaptive OFDM", in *Proceedings of VTC 2003-Fall*, pp. 547 - 551, Vol. 1, Orlando, USA, Oct. 2003.

[3] M. Sternad, T. Ottosson, A. Ahlén and A. Svensson, "Attaining both Coverage and High Spectral Efficiency with Adaptive OFDMA Downlinks", in *Proceedings of VTC 2003-Fall*, pp. 2486 - 2490, Vol. 4, Orlando, USA, Oct. 2003.

[4] W. Wang, T. Ottosson, T. Svensson, A. Svensson and M. Sternad, "Evaluations of a 4G Uplink System Based on Adaptive Single-carrier TDMA", to appear in *Proceedings of VTC 2005-Fall*, Dallas, USA.

[5] M. Sternad and D. Aronsson, "Channel Estimation and Prediction for Adaptive OFDMA/TDMA Uplinks, Based on overlapping Pilots", IEEE ICASSP 2005, Philadelphia, March 19-23, 2005.

[6] T. Pollet, P. Spruyt, and M. Moeneclaey, "The BER performance of OFDM systems using nonsynchronized sampling", in *Proceedings of Globecom*, pp. 253 - 257, Vol. 1, San Francisco, USA, Nov. 1994.

[7] Jan-Jaap van de Beek, Per Ola Börjesson, M. Boucheret, D. Landström, J. M. Arenas, P. Ödling, C. Östberg, M. Wahlqvist and S. K. Wilson, "A Time and Frequency Synchronization Scheme for Multiuser OFDM", *IEEE Journal on selected areas in communications*, pp. 1900 - 1914, vol. 17, No. 11, November, 1999.

[8] M. El-Tanany, Y. Wu and L. Házy, "OFDM Uplink for Interactive Broadband Wireless: Analysis and Simulation in the Presence of Carrier, Clock and Timing Errors", *IEEE Transactions on broadcasting*, pp. 3-19, vol. 47, No. 1, March, 2001.

[9] John G. Proakis, *Digital Communications*, 3rd edition, McGraw-Hill, 1995